

## Dry Deposition of Reactive Nitrogen and Sulfur Compounds in the Greater Seoul Area

Young Sung Ghim<sup>†</sup> and Jin Young Kim

Global Environment Research Center, Korea Institute of Science and Technology,  
P.O. Box 131 Cheongryang, Seoul 130-650, Korea  
(Received 30 April 2001 • accepted 31 July 2001)

**Abstract**—While deposition is a removal process of pollutants from the atmosphere, it is an intake process of such pollutants into the ground. It is suggested that surface waters in the Greater Seoul Area, used as a source of drinking water, have been affected by severe air pollution. In this work, the dry deposition of reactive nitrogen and sulfur species was estimated for three typical days in each season for the year of 1997. The CIT (California Institute of Technology) photochemical model incorporated with a gaseous oxidation reaction of SO<sub>2</sub> was used. The study revealed that reactive nitrogen deposition was the largest in summer and sulfur deposition was the largest in winter. Most of the reactive nitrogen was deposited in the form of HNO<sub>3</sub> and NO<sub>2</sub>, but HNO<sub>3</sub> deposition is highly dependent on the season according to the extent of photochemical production. On the other hand, the contribution of sulfate to the total deposition of sulfur was minimal partly because of low deposition velocity and of the neglect of possible inflow from the boundaries. Approximately 53% of the reactive nitrogen and 30% of the sulfur emitted in the study area was deposited in the ground in the dry form on an annual basis.

Key words: Dry Deposition, Air Quality Modeling, Acidic Compounds, Photochemistry, Seasonal Variation

### INTRODUCTION

The Greater Seoul Area (GSA) - which includes Seoul proper and its neighboring satellite cities - accounts for about 40% of Korea's population but less than 5% of its total land. Seoul, which has an area of 606 km<sup>2</sup>, is crowded with 2.3 million cars and 10 million people. Furthermore, Seoul is surrounded by mountains and hills. There is a low, flat area along the Han River flowing from east to west through the city as shown in Fig. 1. Annual average wind speeds in Seoul are only 2.4 m/s with about 5% calm hours [KMA, 1991], and stable atmospheric conditions occur about 40% of the time. Topography and meteorological conditions as well as high emission density within a small area are unfavorable for air pollutant dispersion. During the 1990s, primary pollutants such as sulfur dioxide and suspended particulate matter have been substantially reduced by aggressive government efforts (e.g., switchover to clean fuel) [Ghim, 1994]. However, the levels of secondary pollutants such as ozone and nitrogen dioxides have tended to increase as a result of the rapidly increasing number of vehicles.

In Korea, more than 90% of drinking water is produced from surface waters including rivers and reservoirs [Park, 1999]. This means that water supply systems are vulnerable to contamination by various pollutants and at risk due to accidents. Recently, it has been suggested that intake water for producing drinking water is affected by air pollutants. Any pollutants in the air can fall and affect the water quality [USEPA, 1999]. Among them, sulfur and nitrogen compounds acidify lakes and streams. Acidification also appears to mobilize toxic metals such as aluminum and mercury. Excess nitrogen can cause eutrophication (over enrichment of nutri-

ents) in nitrogen-sensitive waters such as bays and estuaries, and increase nitrate concentrations in drinking water supplies. It is known that in major rivers of the northeastern U.S., nitrate concentrations have risen three- to ten-fold since the early 1900s, and the evidence suggests a similar trend in many European rivers [Vitousek, 1997].

The major resource of drinking water in the GSA is the Han River shown in Fig. 1. A number of water intake facilities are distributed along the main rivers and their tributaries. In fact, the watershed of the Han River is the largest in Korea, covering almost one fourth of the Korean Peninsula. The size of the airshed affecting the watershed is several times larger than that of the watershed [Dennis, 1997]. However, the domain of 60 km×60 km, centering on Seoul, shown in Fig. 1 is used in the present work in order to investigate the deposition of air pollutants that can affect the water quality of the Han River. This is because major sources of pollutant emissions are conglomerated in this area and, in comparison with other areas, precise information on the emissions is available. For the year of 1997 in the GSA, temporal and spatial variations in dry deposition of sulfur and reactive nitrogen compounds are investigated by using the CIT (California Institute of Technology) Eulerian airshed model [McRae et al., 1992].

Here, reactive nitrogen compounds include nitrogen oxides and their reaction products but do not include reduced nitrogen compounds such as ammonia (NH<sub>3</sub>) and ammonium (NH<sub>4</sub><sup>+</sup>). It is reported that deposition of reduced nitrogen compounds could constitute a considerable fraction of total nitrogen deposition [Fenn and Kiefer, 1999; Tamay et al., 2001]. However, they are not taken into account in this work because both their ambient concentrations and emission amounts are seldom identified in Korea.

<sup>†</sup>To whom correspondence should be addressed.  
E-mail: ysghim@kist.re.kr

### MODELING

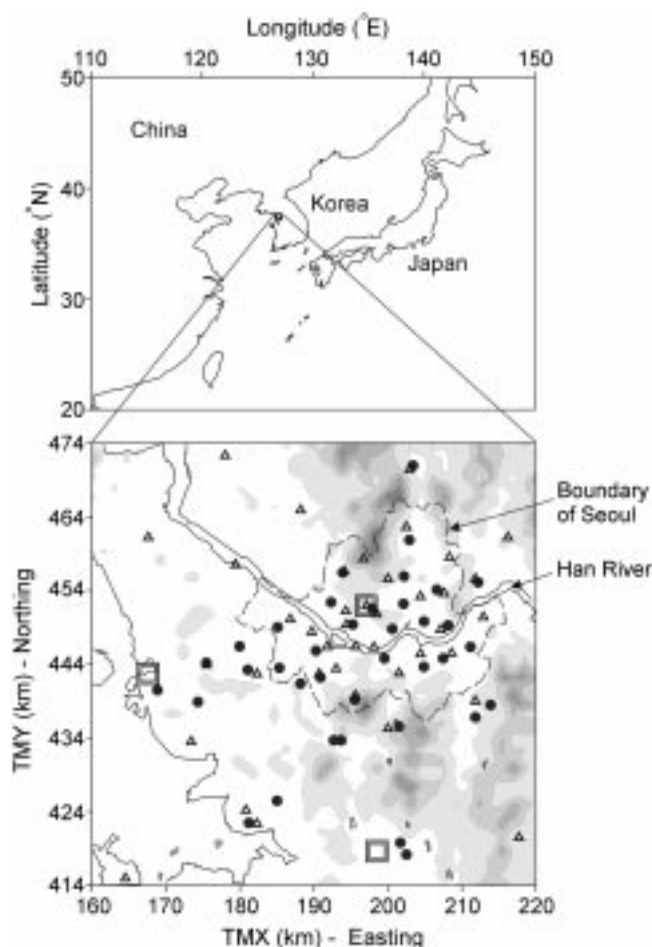


**Fig. 1. Modeling domain and distribution of monitoring stations. Double rectangles denote surface weather stations and open triangles denote automatic weather stations. Solid circles denote air quality monitoring stations. Filled contours represent topography above sea level starting from 50 m at intervals of 100 m.**

## 1. Model Description

The CIT airshed model is an Eulerian photochemical model that solves the atmospheric diffusion equation:

$$\frac{\partial C_i}{\partial t} + \nabla \cdot (\mathbf{u}C_i) = \nabla \cdot (\mathbf{K}\nabla C_i) + R_i \quad (1)$$

where  $C_i$  is the ensemble mean concentration of species  $i$ ,  $\mathbf{u}$  is the wind velocity vector,  $\mathbf{K}$  is the eddy diffusivity tensor,  $R_i$  is the rate of generation of species  $i$  by chemical reactions, and  $t$  is the time. At ground level, the boundary condition is

$$-K_{zz} \frac{\partial C_i}{\partial z} = E_i - v_g^i C_i \quad (2)$$

where  $K_{zz}$  is the vertical eddy diffusivity,  $E_i$  is the emission flux,  $v_g^i$  is the dry deposition velocity for species  $i$ , and  $z$  is the coordinate in the vertical direction. A no-flux boundary condition is applied at the top of the modeling region. Lateral boundary conditions and initial conditions are usually established by using measured concentration data.

The details of the model including numerical solution techniques

can be found elsewhere [Harley et al., 1993; McRae et al., 1982]. However, both chemistry and deposition calculation will be separately described here since the chemistry is slightly altered to estimate the sulfur deposition (sulfur compounds are not major reacting components in an ordinary photochemical reaction system) and the deposition calculation is the key element of this work.

### 1-1. Chemistry

The chemistry is based on the LCC (Lurmann, Carter and Coyner) chemical mechanism, which includes 26 differential and 9 steady-state chemical species [Lurmann et al., 1987]. The only reaction path including sulfur in the CIT model is



However, reaction (R1) leads to a chain mechanism whose final product is sulfate. It is known that there is always enough water vapor in the atmosphere to react with  $\text{SO}_3$  to produce  $\text{H}_2\text{SO}_4$ . Thus, the reaction mechanism including sulfur has been reduced to [Stockwell et al., 1990].



In the present work, reaction (R2) is used instead of (R1) with a rate constant suggested by Carter [1990]. Note that sulfuric acid in reaction (R2) is a gaseous species. However, sulfate in the ambient atmosphere is mostly present in the form of aerosol, either liquid droplet or particulate matter. Therefore, for the deposition velocity of sulfuric acid, a parameterized form of measurements for particulate sulfate by Wesley et al. [1985] is used. Also, the term "sulfate" will be used instead of "sulfuric acid" in this regard.

### 1-2. Calculation of Dry Deposition

In most air quality models, the dry deposition velocity,  $v_g^i$  in Eq. (2) is computed by using a three-resistance scheme that includes aerodynamic resistance due to turbulent transport in the atmospheric boundary layer, laminar sublayer resistance due to molecular diffusion near the surface, and surface resistance due to uptake by the surface elements. In the CIT model, a maximum deposition velocity,  $v_{g,max}$  is first calculated by assuming that the surface acts as a perfect sink:

$$v_{g,max} = k^2 u(z_r) / \left\{ \left[ \int_{z_o}^{z_r} \phi_m \left( \frac{z}{L} \right) \frac{dz}{z} \right] \left[ 2 \left( \frac{Sc}{Pr} \right)^{2/3} + \int_{z_o}^{z_r} \phi_p \left( \frac{z}{L} \right) \frac{dz}{z} \right] \right\} \quad (3)$$

where  $k$  von Karman's constant,  $u(z_r)$  is the wind speed at the reference elevation  $z_r$ ,  $z_o$  is the surface roughness length,  $L$  is the Monin-Obukhov length,  $Sc$  is the Schmidt number, and  $Pr$  is the Prandtl number.  $\phi_m$  and  $\phi_p$  are dimensionless wind shear and concentration gradient in the surface layer, respectively, whose functional form can be obtained from Businger et al. [1971].

Note that the maximum deposition velocity in Eq. (3) is independent of chemical species. This is because  $Sc$  and  $Pr$  are set to be constant, 1.15 and 1.0, respectively, in the model. The species-specific deposition velocity  $v_g^i$  is calculated in terms of  $v_{g,max}$  and a surface resistance:

$$v_g^i = \frac{1}{(1/v_{g,max}) + r_s^i} \quad (4)$$

where  $r_s^i$  is the surface resistance term for chemical species  $i$  that depends on the surface type (i.e., land use) and the solar radiation

**Table 1. Meteorological conditions at the Seoul weather station during the episode days in each season**

Season	Episode days	Average wind speed (m/s)	Average temperature (°C)	Precipitation (mm)	Maximum mixing height (m) <sup>a</sup>
Spring	April 21 to 23	3.2	14.9	-	1,331
Summer	July 27 to 29	1.6	29.4	-	1,312
Fall	Sep. 29 to Oct. 1	1.3	18.2	-	1,282
Winter	January 15 to 17	2.1	-1.8	0.0	1,177

<sup>a</sup>From Chang et al. [1997].

flux.

However, the elevation of the lowest computation grid point is typically much higher than the reference height,  $z_r$ , at which the deposition velocity is defined as shown in Eq. (3). It is necessary to develop an equivalent cell deposition velocity  $\bar{v}_g$  that correctly predicts the flux at the lower boundary when applied to the cell average concentration,  $c_1$ . Since the flux is constant regardless of the height at which the deposition velocity is defined:

$$F = v_g c(z_r) = \bar{v}_g c_1. \quad (5)$$

By assuming that the lowest cell is within the surface layer, along with the concentration gradient form of Businger et al. [1971], the expression for  $\bar{v}_g$  similar to Eq. (3) can be obtained as follows:

$$v_g = \bar{v}_g(z_r) \left[ 1 + \frac{v_g(z_r)}{ku_* (\Delta z - z_r)} \int_{z_r}^{\Delta z} \phi_p \left( \frac{x}{L} \right) \frac{dx}{x} dz \right] \quad (6)$$

where  $\Delta z$  is the depth of the lowest cell and  $u_*$  is the friction velocity. McRae et al. [1982] indicated that the equivalent cell deposition velocity  $\bar{v}_g$  becomes smaller as  $\Delta z$  increases. This means that the concentration decreases with going down to the surface, that is,  $c(z_r) < c_1$  in Eq. (5) due to the deposition loss.

## 2. Model Application to the GSA

The domain of Fig. 1 is horizontally divided into a 2 km×2 km regular grid. Vertically, there are five layers to the model top of 1,100 m. The CIT model uses a terrain-following coordinate system; assuming the sea level, the depth is 38 m at the lowest level and gradually increases. Within the domain, there are 37 air quality monitoring stations, 3 manned surface weather stations and 40 automatic weather stations as shown in Fig. 1. Three consecutive days were

selected as episode days in each season. There was basically no precipitation for five days including the previous two days for spin up; air temperature and wind characteristics were close to those of a normal year [KMA, 1991]. Table 1 shows the meteorological conditions during the episode days observed at the Seoul weather station.

Three-dimensional wind fields were generated diagnostically by using the observations from both manned surface and automatic weather stations along with upper air data. In order to eliminate the boundary effects during the wind field estimation at the surface, the estimation domain was set larger than the study area by 40 km in each direction [Kim et al., 2000]. In constructing the three-dimensional wind field, we used the sounding data from four upper-air stations distributed over the country so that the variations in the upper air over the GSA could coincide with that over the country.

Fig. 2 shows the distributions of  $\text{NO}_x$  and  $\text{SO}_2$  emissions. All sources including area, line, and point sources were combined on the 2 km×2 km grid base. The distribution in Fig. 2 is the same as that prepared by NIER [1994] for the year of 1991 (stationary sources) and 1994 (mobile sources). However, the total amounts were scaled by using the EKMA (Empirical Kinetic Modeling Approach) model [USEPA, 1989] with air quality data at the monitoring stations and measurements of ambient volatile organic compounds (VOC) made in August 1997 [Na et al., 1998]. Because reliable data for diurnal variations of emissions are lacking, a step change in the emission was assumed: 170% of the hourly average emission amounts for 07:00-19:00 LST and 30% of the hourly average emission amounts for the remaining 12 hours after comparing the results with those from a 150-50% change. Also, the same emission data were used

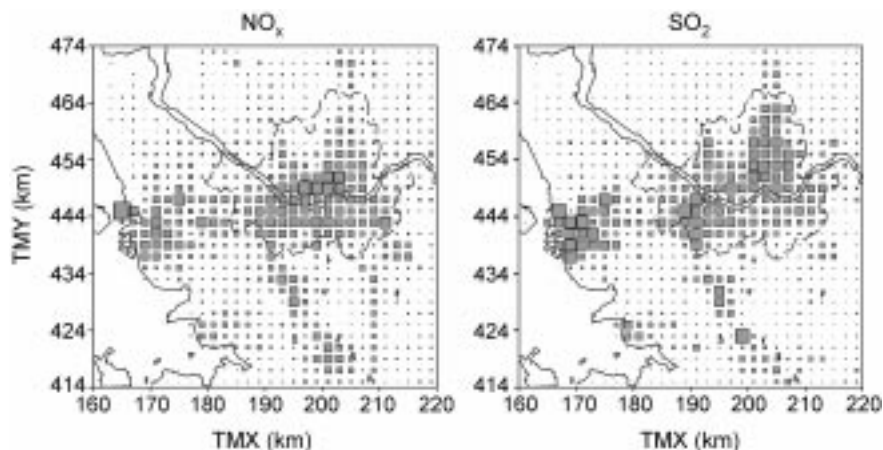


**Fig. 2. Distributions of  $\text{NO}_x$  and  $\text{SO}_2$  emissions. The size of shaded rectangles is proportional to the emission amount. The largest emission is 39 g/s for  $\text{NO}_x$  and 12 g/s for  $\text{SO}_2$ .**

regardless of seasonal change. Therefore, the seasonal variations in the deposition of the current study are mainly caused by meteorology, not by emissions.

In Korea, gaseous species of  $\text{NO}_2$ ,  $\text{SO}_2$ , CO, and ozone are routinely measured as criteria pollutants at the air quality monitoring stations in Fig. 1. These measurement data were used in constructing initial concentration fields and inflow boundary conditions. For VOC concentrations, measurements made in August 1997 [Na et al., 1998] were used by assuming that they were proportional to CO concentrations with the same compositions by considering a close relationship between the two [Kuebler et al., 1996]. Sulfate and nitric acid concentrations were assumed to be zero both initially and at inflow boundaries. Thus concentrations of these species that will be presented in this work are produced entirely within the domain during the modeling period including the spin-up period.

## RESULTS AND DISCUSSION

### 1. Concentration Variations

The predicted concentrations of  $\text{NO}_2$  and  $\text{SO}_2$  are compared with observed ones in Fig. 3. The predicted  $\text{NO}_2$  generally varies in the similar range with the observed one. However, the predicted  $\text{SO}_2$

is two or three times larger than the observed one particularly in the nighttime in summer and fall. A similar phenomenon is also observed in the variation of  $\text{NO}_2$  for the first two days in summer. It is surmised that this is mainly caused by an overestimation of emissions; primary pollutants that were emitted in greater amounts were accumulated at night when wind speeds were low [Kim and Ghim, 2001]. In fact, average wind speeds are just above 1.5 m/s in summer and even lower in fall (Table 1), when the difference between predicted and observed values is large. On the other hand, in the spring of the highest wind speed, the two values coincide well even in the variation of  $\text{SO}_2$ .

It is interesting to note that observed concentrations of both  $\text{NO}_2$  and  $\text{SO}_2$  are higher in winter and spring (Note that the scale of  $\text{SO}_2$  in winter is different). However, these are not distinct in predicted concentrations owing to frequent higher concentrations over observed ones in other seasons. This may be due to seasonal change in real emissions in contrast to the same emissions in the prediction not varying with season. Furthermore, the observed concentrations generally show a peak in the morning; it is not clear in  $\text{NO}_2$  prediction while it is too salient in  $\text{SO}_2$  prediction particularly in winter and fall. It is interpreted that equal diurnal variations for both  $\text{NO}_2$  and  $\text{SO}_2$  emissions assumed in this work cannot produce a peak in the

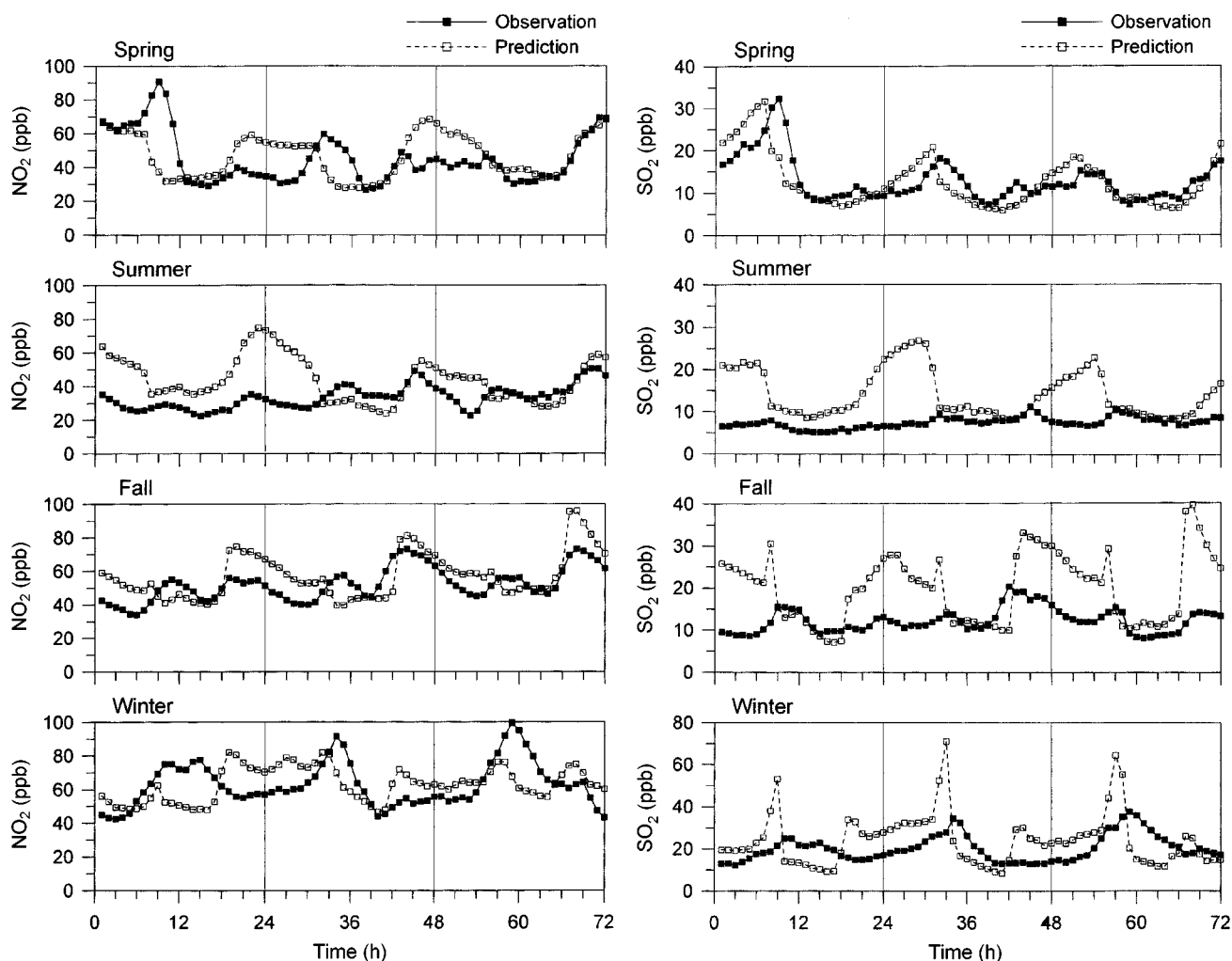


Fig. 3. Comparison of observed and predicted concentrations of  $\text{NO}_2$  and  $\text{SO}_2$ , averaged over the monitoring stations in the domain.

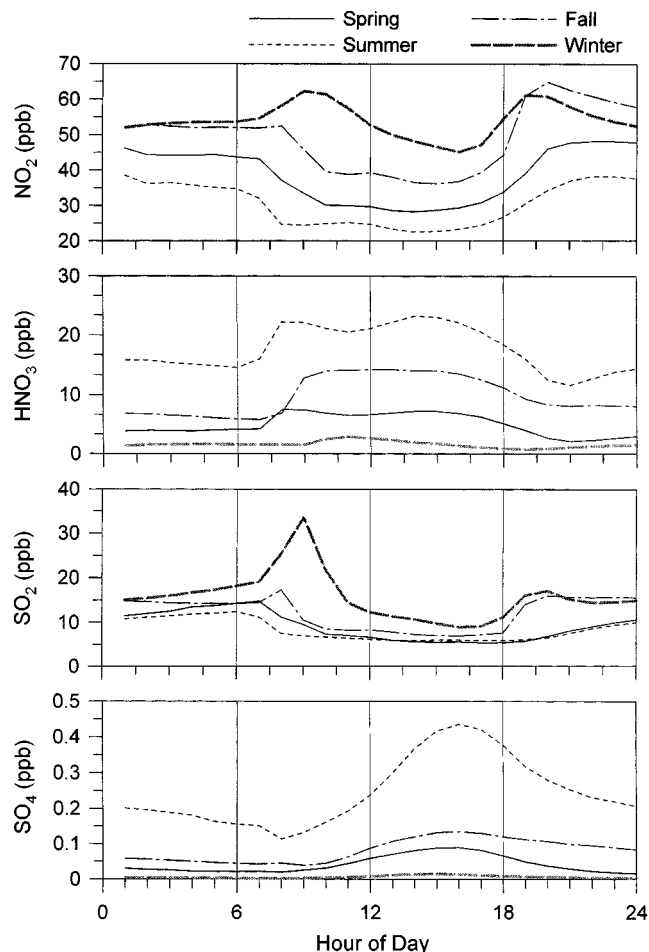


Fig. 4. Variations in the predicted concentration of major species in reactive nitrogen and sulfur deposition averaged over the domain.

morning in  $\text{NO}_2$  prediction while the same diurnal variations produce a salient peak in  $\text{SO}_2$  prediction in winter and fall because it does not closely fit the diurnal variations in real emissions.

Fig. 4 shows temporal variations in predicted concentration of major species in nitrogen and sulfur deposition. Being different from concentrations in Fig. 3 that are averaged over the monitoring stations for comparing the observed ones, concentrations in Fig. 4 are averaged over all grid points in the domain. Diurnal variations are also averaged over the episode days. Concentrations of  $\text{NO}_2$  and  $\text{SO}_2$  are high at night and in winter. This is because these species are principally emitted from the sources and can be accumulated in the stable atmosphere without reaction loss (However, predominantly high concentration of  $\text{SO}_2$  in the morning in winter is mostly caused by inaccurate diurnal variations in emissions as was mentioned earlier.). On the other hand, concentrations of these species are low in the daytime and in summer because of reaction loss and/or because of vertical mixing in the unstable atmosphere.

Lower summertime concentration of  $\text{NO}_2$  compared with those in other seasons indicates that  $\text{NO}_2$  is prone to reaction loss. In the daytime,  $\text{NO}_2$  reacts with hydroxyl radical to produce nitric acid in the presence of the third molecule, M, that absorbs the excess energy [Finlayson-Pitts and Pitts, 1985],

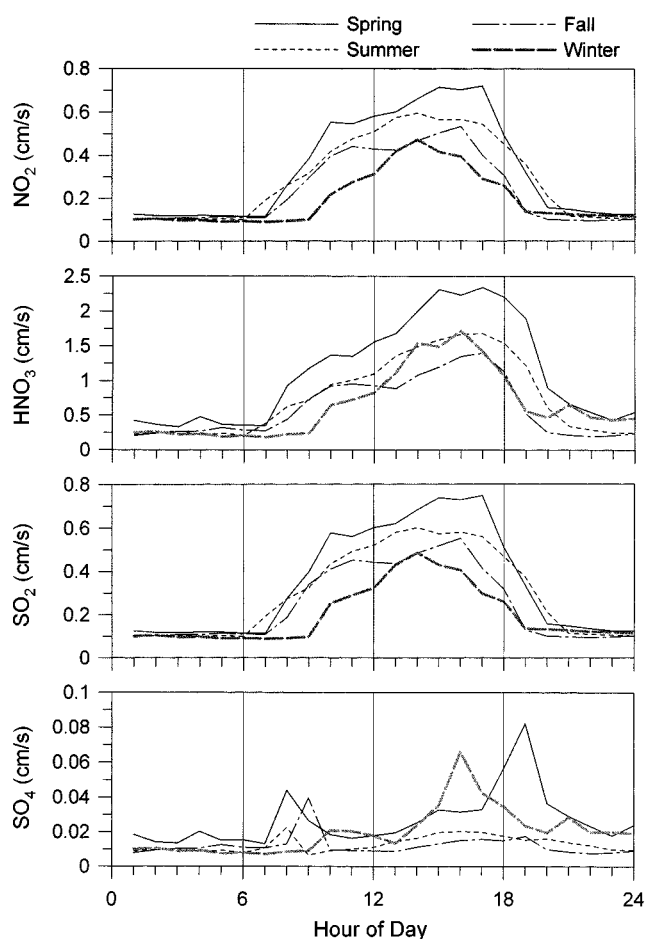


Fig. 5. Variations in the deposition velocity of major species in reactive nitrogen and sulfur deposition averaged over the domain.



As a result, concentration of nitric acid is high in the daytime especially in summer. Concentration of sulfate is also high in the daytime in summer through the reaction (R2). However, its absolute value is much smaller than that of nitric acid, and the reduction of  $\text{SO}_2$  due to reaction (R2) is smaller. As a result, summertime concentration of  $\text{SO}_2$  is comparable to the concentration in spring that is reduced by high wind speed and mixing height.

## 2. Deposition Variations

Fig. 5 shows the variations of the equivalent cell deposition velocities calculated from the deposition flux divided by concentration at the lowest cell, that is,  $F/c_i$  in Eq. (5). Deposition velocity of nitric acid is the highest while that of sulfate is the lowest. The velocities are higher in the afternoon except for sulfate. On the other hand, they are rather constant at night, around 0.3 cm/s for  $\text{HNO}_3$  and 0.1 cm/s for  $\text{NO}_2$  and  $\text{SO}_2$ . Typical winds within a day in the GSA are weak easterlies till morning and strong westerlies in the afternoon [Ghim et al., 2001]. Therefore, it is interpreted that high deposition velocities of  $\text{NO}_2$ ,  $\text{HNO}_3$  and  $\text{SO}_2$  in the afternoon are due to relatively high wind speeds. Furthermore, wind speed is the highest in spring (Table 1) when the deposition velocity is the highest. This indicates that the effect of variations in the aerodynamic resistance

is dominant over those of the other two resistances in the afternoon.

In fact, the aerodynamic resistance of these three species is much larger than the other two resistances at night because the vertical motion of atmospheric turbulence is severely restricted within the stable atmosphere. This is why the deposition velocity is so low at night. However, it decreases in the afternoon along with enhanced vertical mixing and is comparable to the other two resistances. Since the total resistance is small, the deposition velocity becomes higher, and the variation of the aerodynamic resistance that is sensitive to meteorological parameters is manifested.

Fig. 5 shows that the deposition velocity of particulate sulfate is quite different from those of other gaseous species. High deposition velocity in the spring of high wind speed is similar to other species. However, the deposition velocity of particulate sulfate is different in that there are sharp peaks in the diurnal variations and that its value is an order of magnitude lower than that of other species. This is mainly because the surface resistance of sulfate is much larger than those of other species. As a result, the effect of the surface resistance of sulfate is dominant over the other two resistances even in the afternoon, being different from the other species in Fig. 5.

Deposition velocity of each species in Fig. 5 is compared with measurements reported in references in Table 2. As was already mentioned, deposition velocities in Fig. 5 are generally in the lower range, because the deposition velocity in this study is the equivalent cell deposition velocity based on the concentration at the lowest cell (whose height is 38 m at sea level). Nevertheless, deposition velocity of  $\text{NO}_2$  is comparable to typical values suggested by Finlayson-Pitts and Pitts [1985] while that of sulfate is much smaller than the values summarized by Brook et al. [1999].

Deposition fluxes of major species are shown in Fig. 6. In fact, these fluxes are concentrations in Fig. 4 multiplied by deposition velocities in Fig. 5 as shown in Eq. (5). The fluxes of  $\text{NO}_2$ ,  $\text{HNO}_3$  and  $\text{SO}_2$  are large in the daytime both because of high deposition velocities in the afternoon (Fig. 5) and because of high concentrations in the morning (Fig. 4). However, seasonal variations of the flux are not straightforward, mainly because deposition velocities of  $\text{NO}_2$  and  $\text{SO}_2$  are high in summer when their concentrations are low. As a result,  $\text{SO}_2$  flux is generally larger in winter when the concentration is much higher than that in other seasons;  $\text{NO}_2$  flux is generally smaller in summer when the concentration is much lower. On the other hand, nitric acid and sulfate fluxes are simply larger in summer and smaller in winter because both concentration and deposition velocity vary together.

### 3. Deposition Estimation

The deposition amount was calculated at each grid point from

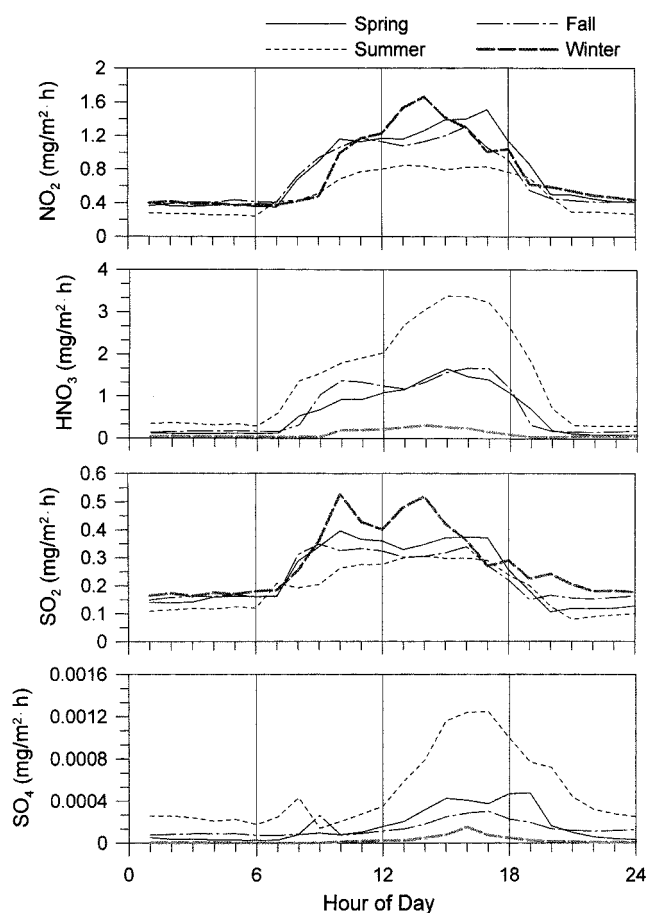


Fig. 6. Variations in the deposition flux of major species in reactive nitrogen and sulfur deposition averaged over the domain.

the deposition flux for three episode days in each season and given in Fig. 7. Deposition of reactive nitrogen is large in the middle, centering on Seoul, where emissions are large (Fig. 2). The distribution is different by season due to meteorological parameters such as wind velocity and air temperature (Note that the same emissions are assumed in all seasons). Deposition of reactive nitrogen is the largest in summer and the smallest in winter. This is due to a great contribution of nitric acid whose flux is large in summer and small in winter (Fig. 6). On the other hand, sulfur deposition is not only large in the middle, similar to reactive nitrogen deposition, but shows a large value along the boundary in spring and winter. This large deposition of sulfur along the boundary is due not to emissions but to

Table 2. Comparison of deposition velocity of major species with measurements

Source	$\text{NO}_2$	$\text{HNO}_3$	$\text{SO}_2$	Sulfate
This study <sup>a</sup>	0.1-0.8	0.2-2.5	0.1 - 0.8	0.01-0.08
Finlayson-Pitts and Pitts [1985]	0.30-0.80 (soil, cement) 1.90 (alfalfa)	1.0-4.7 (grassy field)	0.1-4.5 (grass) 0.1-1.0 (pine forest)	~0.0 (deciduous forest, winter) 0.48-0.90 (pine forest) 0.02-0.42 (grass)
Brook et al. [1999]		0.0-11.0 (forest) 0.0-4.9 (grass)	0.1-2.5 (coniferous forest) 0.1-0.6 (deciduous forest) 0.04-3.4 (grassland)	0.0-4.0 (coniferous forest) 0.0-1.0 (deciduous forest) 0.0-2.5 (grassland)

<sup>a</sup>Equivalent cell deposition velocity for urban, grass and forest.

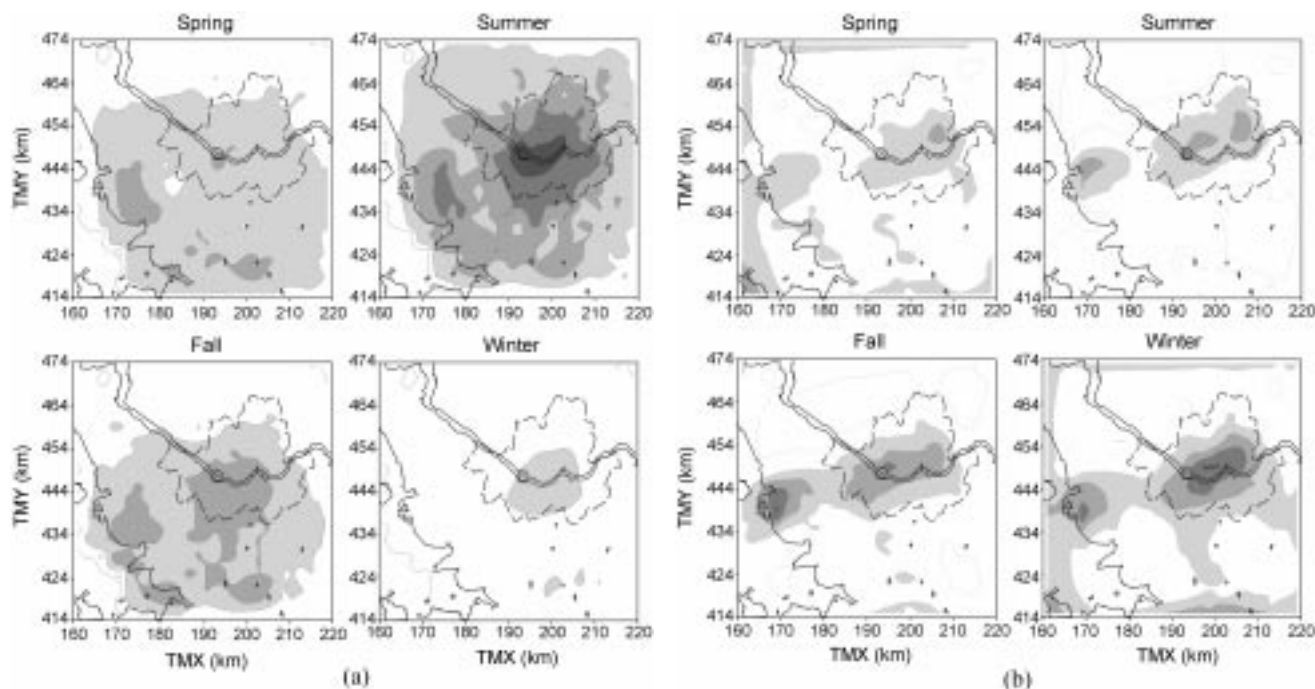


Fig. 7. (a) Distribution of reactive nitrogen deposition for three episode days in each season. (b) Distribution of sulfur deposition for three episode days in each season.

the monitoring data of  $\text{SO}_2$ . In the GSA prevailing wind directions in spring and winter are westerlies. Therefore, as Fig. 7 shows,  $\text{SO}_2$  concentrations are high along the inflow boundaries. This means that more than a small amount of  $\text{SO}_2$  was transported from the outside of the domain.

In the present work, it is assumed that nitric acid and sulfate concentrations are zero at the inflow boundaries. The distributions of deposition in Fig. 7 show that the assumption is plausible for nitric acid, but not for sulfate. This is because a certain amount of sulfate should be present along with  $\text{SO}_2$  at the inflow boundaries [Park and Cho, 1998]. In fact, concentration of sulfate in Fig. 4 is quite small even when compared with that measured at background monitoring sites. Sulfate concentrations were  $0.3\text{--}9\ \mu\text{g}/\text{m}^3$  at islands distant from the GSA and  $4.4\text{--}34\ \mu\text{g}/\text{m}^3$  at an island near the GSA [KIST, 1999]. However, the range of sulfate,  $0\text{--}0.5\ \text{ppb}$  in Fig. 4 corresponds to  $0\text{--}2\ \mu\text{g}/\text{m}^3$ , which is smaller than that at islands with little influence of anthropogenic emissions. Nevertheless, it is true that most of the sulfur dry deposition is accomplished by the deposition of  $\text{SO}_2$ . Recently, Park et al. [2000] estimated that the contribution of sulfate to the total dry deposition of sulfur was less than 5% including the heterogeneous formation.

Table 3 shows total amounts of reactive nitrogen and sulfur deposition for three episode days in each season. As mentioned earlier, deposition of reactive nitrogen is large in summer due to large deposition of nitric acid. However,  $\text{NO}_2$  deposition is larger in spring and fall, and is dominant in winter. It is interesting to note that  $\text{NO}_2$  deposition does not vary much except during the summer when nitric acid is actively produced from  $\text{NO}_2$ . On the other hand, nitric acid deposition is highly dependent on the season according to the extent of photochemical production. In Table 3, almost all of the sulfur deposition is due to  $\text{SO}_2$ . It is thought that this is partly because of the low concentration of sulfate caused by zero inflow boundary

Table 3. Reactive nitrogen and sulfur deposition on nitrogen and sulfur base, respectively, for three episode days in each season (unit: tons). The number in the parentheses represents the percent fraction

Species	Spring	Summer	Fall	Winter
NO	2.6 (2.7)	1.5 (1.3)	4.3 (4.5)	5.4 (7.5)
$\text{NO}_2$	56.9 (58.9)	37.8 (32.4)	52.6 (54.5)	55.3 (76.7)
HONO	0.4 (0.4)	1.0 (0.9)	1.0 (1.0)	0.3 (0.4)
$\text{HNO}_3$	32.3 (33.4)	74.4 (63.9)	36.2 (37.5)	5.9 (8.2)
$\text{N}_2\text{O}_5$	1.1 (1.1)	0.3 (0.2)	0.2 (0.2)	1.5 (2.1)
PAN	3.4 (3.5)	1.5 (1.3)	2.2 (2.3)	3.7 (5.1)
Total	96.7 (100.0)	116.5 (100.0)	96.5 (100.0)	72.1 (100.0)
$\text{SO}_2$	28.3 (100.0)	22.8 (99.8)	27.5 (100.0)	33.8 (100.0)
$\text{SO}_4$	0.0 (0.0)	0.05 (0.2)	0.0 (0.0)	0.0 (0.0)
Total	28.3 (100.0)	22.85 (100.0)	27.5 (100.0)	33.8 (100.0)

conditions and partly because of low deposition velocity (Table 2) in the present work. If the emissions in Fig. 2 are summarized, annual emissions of nitrogen and sulfur in the GSA are 21,700 tons and 11,300 tons, respectively. It can be estimated that annual depositions of reactive nitrogen and sulfur are 11,600 tons and 3,400 tons from Table 3. This indicates that 53% of the reactive nitrogen emitted and 30% of the sulfur emitted was deposited in the dry form on an annual basis.

## CONCLUSIONS

The reactive nitrogen and sulfur deposition over the Greater Seoul Area (GSA) was estimated by using an Eulerian airshed model for three episode days in each season in 1997. Since both emission

amounts and diurnal variations were not changed by season, the variations in the work were mainly caused by meteorological parameters along with some contribution of air quality monitoring data at the boundaries. The deposition of gaseous species was large in the daytime partly because of high deposition velocity in the afternoon and of high concentrations in the morning. The deposition of primary pollutants such as  $\text{NO}_2$  and  $\text{SO}_2$  was large in winter while that of the secondary pollutants such as nitric acid and sulfate was large in summer.

A substantial amount of  $\text{NO}_2$  was converted to nitric acid in summer afternoon and was deposited. As a result, reactive nitrogen deposition was the largest in summer and more than 60% of it was in the form of nitric acid. On the other hand, sulfur deposition was the largest in winter; the contribution of sulfate was minimal even in summer. It is known that sulfate does not contribute much to sulfur deposition [Park et al., 2000]. However, the sulfate contribution in this work was considered too small because the deposition velocity was particularly lower than the measurements and also because the possible inflow from the boundary was neglected.

In the case of the GSA, more elaboration was needed in order to increase the accuracy in the estimation of sulfur deposition. This is different from the common understanding that an accurate estimation of nitrogen deposition is difficult because of complex photochemistry in which a large number of species are involved [Dennis, 1997]. Although only homogeneous gas-phase reactions were considered in the present work, it is surmised that involvement of particulate nitrate increases nitrogen deposition especially in winter because it could help produce more nitric acid (Note that ammonium nitrate, a common form of particulate nitrate in urban areas, is easily dissociated at higher temperatures [Seinfeld and Pandis, 1998]). Finally, it is certain that ambiguity could be greatly reduced just with more information on temporal, both seasonal and diurnal, variations in the emission.

### ACKNOWLEDGMENTS

This work was carried out as a part of Green Korea 21 of the Korea Institute of Science and Technology.

### NOMENCLATURE

$C_i$	: ensemble mean concentration of species $i$
$c_1$	: average concentration at the lowest cell
$E_i$	: emission flux of species $i$
$F$	: deposition flux
$\mathbf{K}$	: turbulent eddy diffusivity tensor
$k$	: von Karman's constant
$K_{zz}$	: vertical eddy diffusivity
$L$	: Monin-Obukhov length
$Pr$	: Prandtl number
$R_i$	: rate of generation of species $i$ by chemical reactions
$r_s^i$	: surface resistance for species $i$
$Sc$	: Schmidt number
$\mathbf{u}$	: wind velocity vector
$u$	: wind speed
$u_*$	: friction velocity
$\bar{V}_g$	: equivalent cell deposition velocity

$V_g^i$	: dry deposition velocity for species $i$
$V_{g,max}$	: maximum deposition velocity when the surface acts as a perfect sink
$t$	: time
$z$	: coordinate in the vertical direction
$z_o$	: surface roughness length
$z_r$	: reference height used to establish the deposition velocities
$\Delta z$	: depth of the lowest cell

### Greek Letters

$\phi_m$	: dimensionless wind shear in the surface layer for momentum transport
$\phi_p$	: dimensionless concentration gradient in the surface layer for pollutant transport

### REFERENCES

- Brook, J. R., Zhang, L., Li, Y. and Johnson, D., "Description and Evaluation of a Model of Deposition Velocities for Routine Estimates of Dry Deposition over North America. Part II: Review of Past Measurements and Model Results," *Atmospheric Environment*, **33**, 5053 (1999).
- Businger, J. A., Wyngaard, J. C., Izumi, Y. and Bradley, E. F., "Flux-Profile Relationships in the Atmospheric Surface Layer," *J. Atmospheric Sciences*, **28**, 181 (1971).
- Carter, W. P. L., "A Detailed Mechanism for the Gas-Phase Atmospheric Reactions of Organic Compounds," *Atmospheric Environment*, **24A**, 481 (1990).
- Chang, Y.-S., Brown, D. F. and Ghim, Y. S., "Estimation of Mixing Heights Using the Holzworth Method in Korea," *J. Korea Air Pollution Res. Assoc.*, **13**(E), 35 (1997).
- Dennis, R. L., "Using the Regional Acid Deposition Model to Determine the Nitrogen Deposition Airshed of the Chesapeake Bay Watershed," *Atmospheric Deposition of Contaminants to the Great Lakes and Coastal Waters*, Baker, J. E., ed., SETAC Technical Publications Series, Society of Environmental Toxicology and Chemistry (SETAC), Pensacola, FL (1997).
- Fenn, M. E. and Kiefer, J. W., "Throughfall Deposition of Nitrogen and Sulfur in a Jeffrey Pine Forest in the San Gabriel Mountains, Southern California," *Environ. Pollution*, **104**, 179 (1999).
- Finlayson-Pitts, B. J. and Pitts, J. N., "Atmospheric Chemistry: Fundamentals and Experimental Techniques," Wiley-Interscience, New York (1985).
- Ghim, Y. S., "Air Quality Changes in Seoul as a Result of Switchover to Clean Fuel," (in Korean), *Chemical Industry and Technology*, **12**, 303 (1994).
- Ghim, Y. S., Oh, H. S. and Chang, Y.-S., "Meteorological Effects on the Evolution of High Ozone Episodes in the Greater Seoul Area," *J. Air Waste Manage. Assoc.*, **51**, 185 (2001).
- Harley, R. A., Russel, A. G., McRae, G. J., Cass, G. R. and Seinfeld, J. H., "Photochemical Modeling of the Southern California Air Quality Study," *Environ. Sci. Tech.*, **27**, 378 (1993).
- Kim, J. Y., Ghim, Y. S., Kim, Y. P. and Dabdub, D. D., "Determination of Domain for Diagnostic Wind Field Estimation in Korea," *Atmospheric Environment*, **34**, 595 (2000).
- Kim, J. Y. and Ghim, Y. S., "Effects of the Density of Meteorological Observations on the Diagnostic Wind Fields and the Performance

- of Photochemical Modeling in the Greater Seoul Area," submitted for publication in *Atmospheric Environment* (in revision) (2001).
- KIST (Korea Institute of Science and Technology), "Study on Long-range Transport of Air Pollutants in Northeast Asia (IV)," (in Korean), Report to the National Institute of Environmental Research, Seoul, Korea (1999).
- KMA (Korea Meteorological Administration), "Climatological Standard Normals of Korea," (in Korean), Vol. II, Seoul, Korea (1991).
- Kuebler, J., Giovannoni, J.-M. and Russel, A. G., "Eulerian Modeling of Photochemical Pollutants over the Swiss Plateau and Control Strategy Analysis," *Atmospheric Environment*, **30**, 951 (1996).
- Lurmann, F. W., Carter, W. P. and Coyner, L. A., "A Surrogate Species Chemical Reaction Mechanism for Urban-Scale Air Quality Simulation Models," Volumes I and II, Report to the U.S. Environmental Protection Agency under Contract 68-02-4104, ERT Inc., Newbury Park, CA and Statewide Air Pollution Research Center, University of California, Riverside, CA (1987).
- McRae, G. J., Goodin, W. R. and Seinfeld, J. H., "Development of a Second-Generation Mathematical Model for Urban Air Pollution-I. Model Formulation," *Atmospheric Environment*, **16**, 679 (1982).
- McRae, G. J., Russell, A. G. and Harley, R. A., "CIT Photochemical Airshed Model," California Institute of Technology, Pasadena, CA (1992).
- Na, K. S., Kim, Y. P. and Moon, K. C., "Characteristics of Concentrations of C<sub>2</sub>-C<sub>9</sub> Hydrocarbons in Urban and Industrial Locations in Ambient Air," (in Korean), Abstract SM5, Fall Meeting of the Korea Air Pollution Research Association, Kyongsan, Korea (1998).
- NIER (National Institute of Environmental Research), "A Study on Visibility and Smog Phenomena in Seoul Metropolitan Area (I)," (in Korean), Seoul, Korea (1994).
- Park, W. H., "Koreas Environmental Management of Water Resources and Water Quality," 6<sup>th</sup> Workshop on Environment Protection Technology Management, Korea Institute of Science and Technology in Association with Korea International Cooperation Agency, Seoul, Korea (1999).
- Park, J. and Cho, S. Y., "A Long Range Transport of SO<sub>2</sub> and Sulfate between Korea and East China," *Atmospheric Environment*, **32**, 2745 (1998).
- Park, S.-U., In, H.-J., Kim, S.-W. and Lee, Y.-H., "Estimation of Sulfur Deposition in South Korea," *Atmospheric Environment*, **34**, 3259 (2000).
- Seinfeld, J. H. and Pandis, S. N., "Atmospheric Chemistry and Physics from Air Pollution to Climate Change," Wiley-Interscience, New York (1998).
- Stockwell, W. R., Middleton, P., Chang, J. S. and Tang, X., "The Second Generation Regional Acid Deposition Model Chemical Mechanism for Regional Air quality Modeling," *J Geophys. Res.*, **95**, 16, 343 (1990).
- Tamay, L., Gertler, A. W., Blank, R. R. and Taylor, G. E., Jr., "Preliminary Measurements of Summer Nitric Acid and Ammonia Concentrations in the Lake Tahoe Basin Air-shed: Implications for Dry Deposition of Atmospheric Nitrogen," *Environ. Pollution*, **113**, 145 (2001).
- USEPA (U.S. Environmental Protection Agency), "Procedures for Applying City-Specific EKMA," EPA-450/4-89-012, Research Triangle Park, NC (1989).
- USEPA (U.S. Environmental Protection Agency), Oceans and Coastal Protection Division, <http://www.epa.gov/OWOW/oceans/airdep/> (accessed in January 2001) (1999).
- Vitousek, P. M., Aber, J., Howarth, R. W., Likens, G. E., Matson, P. A., Schindler, D. W., Schlesinger, W. H. and Tilman, G. D., "Human Alteration of the Global Nitrogen Cycle: Causes and Consequences," <http://esa.sdsc.edu/tilman.htm> (accessed in January 2001) (1997).
- Wesley, M. L., Cook, D. R., Hart, R. L. and Speer, R. E., "Measurements and Parameterization of Particulate Sulfur Dry Deposition over Grass," *J. Geophys. Res.*, **90**, 2131 (1985).